COMPARISON OF MELT-COMPOUNDED NANOCOMPOSITES OF ATOMIC-LAYER-DEPOSITION-COATED POLYAMIDE PARTICLES AND COMMERCIAL NANOFILLERS

Katja Nevalainen[1], Christian Hintze[2], Reija Suihkonen[1], Janne Sundelin[1], Pirkko Eteläaho[1], Jyrki Vuorinen[1], Pentti Järvelä[1] and Nora Isomäki[3]

[1] DEPARTMENT OF MATERIALS SCIENCE, TAMPERE UNIVERSITY OF TECHNOLOGY
P.O. Box 589, FI-33101 Tampere, Finland
katja.nevalainen@luukku.com

[2] DEPARTMENT OF MECHANICAL ENGINEERING, TECHNICAL UNIVERSITY OF CHEMNITZ
P.O. Box 589, D-09107 Chemnitz, Germany

[3] BENEQ OY
P.O. Box 46, FI-02201 Espoo, Finland

ABSTRACT

This paper compares polyamide nanocomposites prepared from atomic-layer-deposition-(ALD)-coated polyamide particles and commercial titanium dioxide nanofillers. In the former case, micron-sized polyamide particles were coated with a thin titanium dioxide film by ALD technology. The thickness of the ALD film was evaluated with a scanning electron microscope using an energy dispersive spectrometer. Particles with titanium oxide shells were melt-compounded to form polyamide nanocomposites similarly to the traditional powder mixture of polyamide and nanofillers. The degree of dispersion in the nanocomposites was characterized with a transmission electron microscope. Furthermore, the specimens were analyzed in rheological and thermal tests to determine their properties. Results showed that a morphology very different from that of the traditionally filled polyamide nanocomposite was obtained for the extruded ALD-coated polyamide particles. Furthermore, the complex viscosity of the ALD nanocomposite was significantly lower than that of the conventionally nanofilled or pure polyamide. The effect of these changes on the processing characteristics of polyamide nanocomposites are discussed in terms of thermal properties.

1 INTRODUCTION

In a polymeric nanocomposite, highly dispersed nanofillers can yield significantly better barrier, mechanical, and thermal properties than conventionally filled polymers. Two common approaches to form polymer nanocomposites are melt-compounding and in-situ polymerization. In the former, nanofiller particles are mixed into a melted polymer matrix at high shear, whereas in the latter, polymerization of the matrix occurs in the presence of nanofillers. Despite extensive research on polymer nanocomposites, it is difficult to produce good adhesion between filler and polymer matrix along with good dispersion of the nanofiller [1,2]. Consequently, there is a clear need to chemically bond nanofillers and polymer and to disperse nanofillers more homogeneously throughout the polymer matrix to gain the desired polymer nanocomposite properties.

In recent years, atomic layer deposition (ALD) has been used in subnanometer coatings on inorganic nano- and microscale particles. The first report on the ALD method to coat particles appeared in the United States in 1999, followed eventually by a U.S. patent [3]. As a result, intensive research has focused on ALD coating of a number of different particle sizes and types such as titania, silica, and iron oxide [3,4]. ALD technology enables tailoring the particle surface chemistry to optimize, for example, the particle-polymer interaction. In principle, ALD is a gas-phase chemical process, which produces extremely thin films of inorganic materials. Typically, two chemicals are used to create alternate, saturated, chemical reactions virtually on any substrate surface. The

process sequentially introduces reactants to substrate surfaces in the gas phase to build successive film monolayers.
ALD is also a convenient technology to produce polymeric nanocomposites. A new method has been developed to promote dispersion of polymer nanocomposites by precoating polymer particles with ultra thin inorganic films through particle ALD and subsequent melt-compounding. Successful results have been obtained with particles of high density polyethylene coated with nanoscale alumina. Upon extrusion, high shear breaks the inorganic shells and disperses the shell remnants to form a nanocomposite with homogenous dispersion of the inorganic filler [4,5]. This approach to nanocomposite fabrication is very attractive in terms of improved dispersion of the nanofiller, but only a few studies exist and none, to our knowledge, on the rheological and thermal properties of such nanocomposites. Ours is a study of melt-compounded titanium dioxide polyamide nanocomposites. The objective was to compare ALD-coated polyamide particles and traditional nanofillers and thus provide further insight into the application of ALD technology as a means of introducing nanofillers into a polymer matrix.

2 EXPERIMENTS

2.1 Materials and ALD coating of polyamide particles

The polymeric powder used was polyamide PA2200 (EOS GmbH) with an average particle size of 60 μm [6]. Ultra thin films of TiO_2 were laid on polyamide particles in a commercial ALD reactor, manufactured by Beneq Oy and illustrated schematically in Figure 1. In the procedure, the PA powder (c. 100 g per coating cycle) was positioned on a filter-covered plate (Ø 200 mm) and mounted in the ALD chamber. Titanium tetrachloride ($TiCl_4$) and water (H_2O) were used as precursors to form TiO_2 films, and high purity nitrogen (N_2) gas led the precursor vapour into the ALD chamber. The reaction temperature and pressure were fixed at 40°C and 1.3 mbar, respectively. The growth sequence consisted of a 30-s pulse of water vapour, followed by a 15-s N_2 purge, then a 60-s pulse of $TiCl_4$ and another 15-s N_2 purge. This sequence was repeated as many times as necessary to deposit TiO_2 films of an approximate nominal thickness of 10 nm and 40 nm on the PA particle substrate. Details of the chemical reactions occurring in the ALD process on different substrates have been reported elsewhere [7,8]. In the process we used, the pulsing times were extended beyond those used in conventional ALD coating to ensure effective film formation on the PA particles.

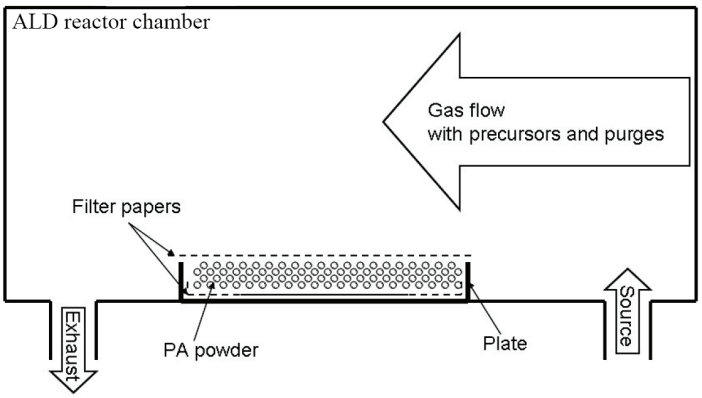

Figure 1: Schematic of the ALD reactor chamber where polyamide (PA) powder was coated with TiO_2.

For comparison, two commercial TiO_2 nanofillers were selected, namely, Aeroxide P25 and T805, supplied by Degussa (Table 1). The P25 has an untreated, hydrophilic surface, whereas that of the T805 is modified with octylsilane.

Table 1: Physical properties and identification of studied materials [6,9].

Identification	Material	Trade name	Supplier	Particle size (nm)	Density (g/cm^3)
PA	Polyamide 12 powder	Eosint P PA 2200	EOS GmbH	~ 60 000	1.0
PA 0.5wt.% ALD	Polyamide 12 powder coated with 10 nm TiO_2 layer by ALD[a]	-	EOS GmbH & Beneq Oy	~ 60 000	-
PA 1.5wt.% ALD	Polyamide 12 powder coated with 40 nm TiO_2 layer by ALD[a]	-	EOS GmbH & Beneq Oy	~ 60 000	-
P25	Unmodified nano-TiO_2	Aeroxide TiO_2 P25	Degussa GmbH	21	3.8
T805	Octylsilane modified nano-TiO_2	Aeroxide TiO_2 T805	Degussa GmbH	21	3.5

[a] TiO_2 thin film on the PA 2200 particles was manufactured in a Beneq Oy commercial ALD reactor.

2.2 Melt-compounding and injection moulding

Prior to each processing step, composite materials were oven-dried at 80°C for several hours. The PA was melt-compounded in a 5-cm^3 DSM microextruder, operating at 220°C and 200 rpm with 2-minute dwell time. Specimens with 2 wt.% filler content were prepared from commercial TiO_2 fillers, whereas the ALD-coated PA particles were melt-compounded as received from the ALD reactor, yielding about 0.5 wt.% for the 10-nm and 1.5 wt.% for 40-nm thin-film-coated PA particles. In these calculated approximations, density values of 0.95 g/cm^3 [6] for PA and 3.5 g/cm^3 [10] for TiO_2 were used. Subsequent injection moulding of the test specimens was done using a 5-cm^3 DSM injection moulding machine, operating at an injection pressure of 3.5 bar, a barrel temperature of 220°C, and a mould temperature of 80°C.

2.3 Sample characterization and analytical methods

The studied polyamide powders were examined with a scanning electron microscope (SEM), using a Philips-XL 30 apparatus operating at an accelerating voltage of 10 kV. Compositional data of the ALD film on the PA particles was obtained with an energy dispersive spectrometer (EDS) Edax DX-4. Prior to the SEM studies, the specimens were coated with a thin carbon layer using a vacuum evaporator to avoid charging.

Rheological measurements were carried out by using a rotational rheometer (Physica MCR 301). Rotational rheometry experiments were run with a parallel-plate geometry and coin shaped samples (Ø 25 mm, thickness 1.5 mm). A temperature/frequency sweep method was selected, and the frequency range was 0.1–550 rad/s at 200 °C. The strain rate was taken as 1%. All samples were oven-dried at 80 °C for several hours and then tested under a continuous nitrogen purge to prevent moisture-induced and oxidative degradation of PA.

Differential scanning calorimetry (DSC) was performed using a Netzsch DSC 204 F1, operating under nitrogen. Extruded and injection-moulded samples of about 10 mg were dried in a vacuum oven prior to experiment. The heating-cooling cycle was repeated three times. The cycles were recorded from -20 to 200°C at a scanning rate of

10°C/min under nitrogen. Before cooling runs, the samples were held for about 3 minutes at 200°C to erase their thermal history. The degree of crystallinity (χ_c) was evaluated from the first heating run to reflect the state of the material after moulding. The degree of the crystallinity phase was determined from the ratio of the heat of fusion of the specimen and the heat of fusion of 100% crystalline PA 12 (209.1 J/g) [11,12].

Dynamic mechanical analysis (DMA) was conducted using a Perkin Elmer Pyris Diamond DMA, operating in single cantilever mode at an oscillation frequency of 1.0 Hz at a temperature of -80 to 110°C. Measurements were performed under nitrogen at 2°C/min heating rate. Specimens with approximate dimensions of 10 x 5 x 2 mm^3 were cut from injection-moulded tensile bars (1BA test bar according to SFS-EN ISO 527-2), and their edges and surfaces were polished with sandpaper. The storage modulus (E'), the loss modulus (E''), and the loss factor (tan δ), were determined.

The dispersion of the ALD-created TiO_2 coating and the traditional fillers within the melt-compounded polyamide matrix was examined with a TEM (JEOL model JEM 2010) operating at an accelerating voltage of 120 kV. The TEM specimens were about 60 nm thick and prepared with a Leica Ultracut UCT at room temperature. The specimens were post-stained with uranyl acetate and lead citrate.

3 RESULTS

3.1 Characterization of materials prior to melt-compounding

Characterization performed with the SEM showed extensive variation in the particle size of PA (Figure 1a) with particle dimensions ranging between 20 – 90 μm. The average particle diameter was, however, close to the nominal value of 60 μm [6].

The amount of TiO_2 on the ALD-coated PA particles was evaluated by means of back scattered electrons (BSE) in the SEM. Whereas the BSE images of the pure PA particles showed no pronounced contrast variation (Figure 2a), the particles coated with 10 nm TiO_2 (Figure 2b) showed clear contrast variation between different particles. With particles coated with 40 nm TiO_2, the change in contrast was even greater (Figure 2c). Contrast variation implies variation in the thickness of TiO_2. The result was confirmed with an EDS: the darkest particles contained no titanium at all, whereas the brightest particles contained the most titanium.

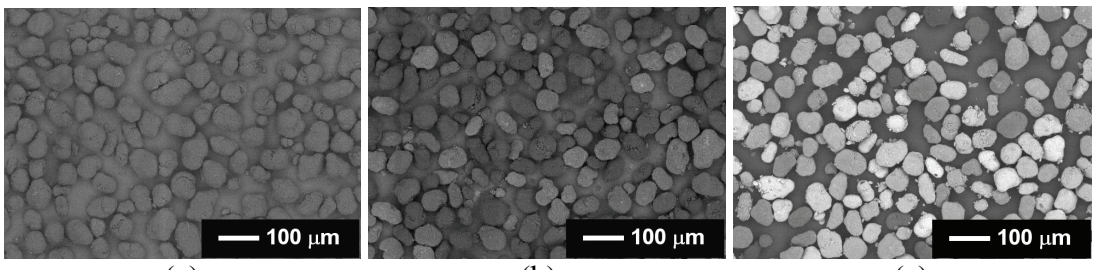

(a) (b) (c)

Figure 2. SEM images of (a) pure PA powder, (b) PA powder coated with 10 nm TiO_2 (PA 0.5 wt% ALD), and (c) PA powder coated with 10 nm TiO_2 (PA 1.5 wt% ALD), where backscattered electrons were used for image formation.

3.2 Rheological properties of nanocomposites

ALD- and traditionally filled nanocomposites were melt-compounded in the DSM microextruder. During processing, DSM screw torsional resistance data was collected, revealing significant differences in the processing behaviour of the studied materials

(Figure 3a). The results suggest that the screw torsional resistance, and hence shear viscosity, of PA ALD composites is abruptly lower than that of a traditionally TiO_2-filled (P25 and T805) and pure PA matrix.

A deeper insight into this interesting shear flow behavior of the studied nanocomposites was gained from rheological measurements (see Figure 3b for the complex viscosity during dynamic shear rheological tests at 200°C). The results demonstrate that the complex viscosity of PA increased slightly in the presence of commercial TiO_2 fillers (P25 and T805), as suggested by the screw torsional resistance values (Figure 3a). Traditionally filled TiO_2 composites exhibit more intensive shear thinning behaviour than pure PA, which indicates that commercial TiO_2 fillers impede the mobility of the polymer chains. Such behaviour in nanofilled polymercomposites is often explained by the homogeneous dispersion of the nanometer-scale particles and by strong interfacial interactions between polymer and filler [13]. Apparently, at low shear rates, TiO_2 agglomerates separate, thus increasing the viscosity of the melt. At higher shear rates, on the other hand, the agglomerates break up and form a more homogenous matrix, and/or they are oriented in the flow direction, thus reducing viscosity.

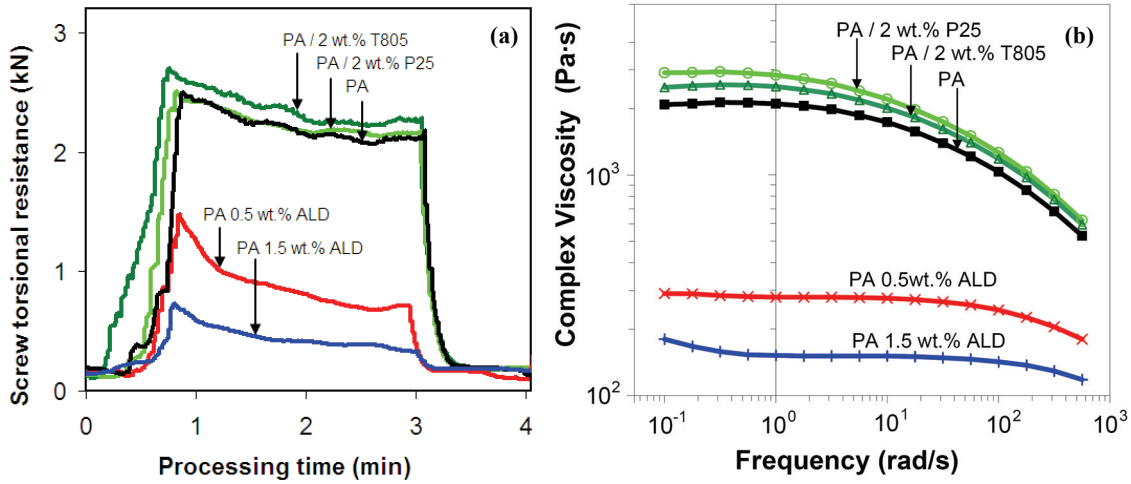

Figure 3: (a) DSM screw torsional resistance (compound dwell time in screw was approximately 2 minutes) as a function of processing time and (b) complex viscosity as a function of frequency for PA / TiO_2 nanocomposites at 200°C.

A significantly lower viscosity of the PA ALD nanocomposite was confirmed in the rheological measurements (Figure 3b). It is not clear what mechanism caused such a reduction in the melt viscosity. A low viscosity in the molten state of, e.g., PA nanoclay composites is generally associated with three factors. The first factor is the slippage of polymer chains over nanoclay platelets during shear flow [12]. Second, the organic molecules used to modify the filler particle could partially enter the matrix and reduce viscosity. The third factor, suggested by a number of researchers, is due to the molecular weight reduction as a result of the degradation and chain scission of the polymer matrix during melt-compounding [12,14]. Because PA ALD nanocomposites contain no modifier, the low viscosity of PA may result from polymer chains slipping over TiO_2 during shear flow or from the reduced PA molecular weight.

3.3 Thermal properties of nanocomposites

Thermal properties such as the glass transition temperature (T_g) depend, among other things, on molecular weight and the extend of the branching and crosslinking of the

polymer matrix and on other factors such as polymer chemical structure, amount of fillers, and measurement conditions [15]. Because T_g depends on the molecular weight of the polymer matrix [16], comparison of DSC and DMA results was seen as a fast and effective way to assess molecular weight changes in the specimens and further explain the unexpected rheological behaviour of the nanocomposites.

The DSC curves of the nanocomposites (Figure 4) suggest that a small amount of nanofillers, both traditional and ALD-created, does not affect the thermal behaviour of polyamide over a wide temperature range. Allowing for instrument errors, we can see from Table 2 that the degree of crystallinity (χ_c) and melting temperature (T_m) of the host matrix did not change significantly even during the three DSC heating cycles. Furthermore, only couple of degrees increase in T_g is recorded upon addition of ALD-created TiO_2. The DSC results, however, revealed that the crystallization peak temperature (T_c) of either pure PA or its commercial nano-TiO_2 composites was around 164–167°C, whereas the T_cs of ALD nanocomposites shifted to 158–160°C. Generally, the function of the particles in nanocomposites is to decrease the crystallite size and increase the crystallization temperature [17], but this was not demonstrated in our work. Furthermore, complex melting behaviors were observed. During the second and third heating at 10°C/min, one major peak with a shoulder and / or second minor peak on the left-hand side appeared at around 170°C. This could be explained by changes in the form of the crystals due to ALD-created TiO_2, as also other authors have found for a PA 6 / nanoclay matrix [18]. Such behaviour could originate from the different melting behaviour of two dissimilar crystalline phases, namely, crystallized amorphous phase and recrystallization of crystalline phase in PA detected by the glass transition peak and melting peak in the first heating, respectively.

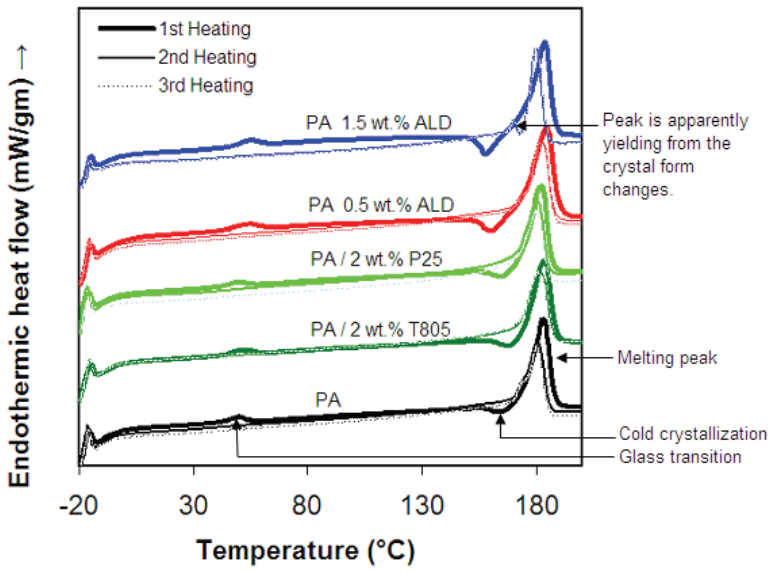

Figure 4: DSC curves for PA / TiO_2 nanocomposites.

DSC results on commercial nanofillers agree well with previous studies of PA 6 / TiO_2 nanocomposites [19]. It seems that crystallinity, T_g and T_m, does not significantly depend on either commercial TiO_2 content or ALD-created TiO_2 content. Thus the DSC results suggest that degree of crystallinity and the degradation of the PA matrix had only a minor effect on the changes observed in the rheological properties of PA ALD composites.

Table 2: Summarized DSC results for PA / TiO_2 nanocomposites.

Material	1st Heating[b]				2nd Heating[b]		3rd Heating[b]	
	χ_c[a] (%)	T_g (°C)	T_c (°C)	T_m (°C)	T_g (°C)	T_m (°C)	T_g (°C)	T_m (°C)
PA	24	47	164	183	36	181	40	180
PA 0.5wt.% ALD	26	49	160	185	40	182	42	182
PA 1.5wt.% ALD	23	51	158	184	-	180	-	180
PA / 2 wt.% T805	20	48	167	184	-	182	-	181
PA / 2 wt.% P25	22	45	164	183	-	180	-	180

[a] Determined from the ratio of the specimen ΔH_m and the heat of fusion of 100% crystalline PA 12 (209.1 J/g) [11,12].
[a] T_g taken from the T_g inflection point , T_c from the exotherm minimum, and T_m values from the DSC melting peak maximum.

Dynamic mechanical properties can provide further information about the viscoelastic behavior of the nanocomposites. Figure 5a shows the storage modulus (E') as a function of temperature for the prepared samples where, in the 30–65°C range, the dramatic E' drop demonstrated the glass transition of PA. The E' values for the T805 TiO_2-filled and the ALD composites are 7–14% higher than for pure PA, whereas for the P25 composites the E' curve is almost identical to pure PA. The increase of storage modulus above mentioned composites resulted apparently from strong interfacial interactions between polymer and surface modified TiO_2 particles (T805) and ALD-created TiO_2. Reason for this behaviour is the reduced mobility of polymer chains, increased modulus of nanocomposite due to the inherent high modulus of TiO_2. Similar results have been obtained for PA 6 / nanoclay composites [20].

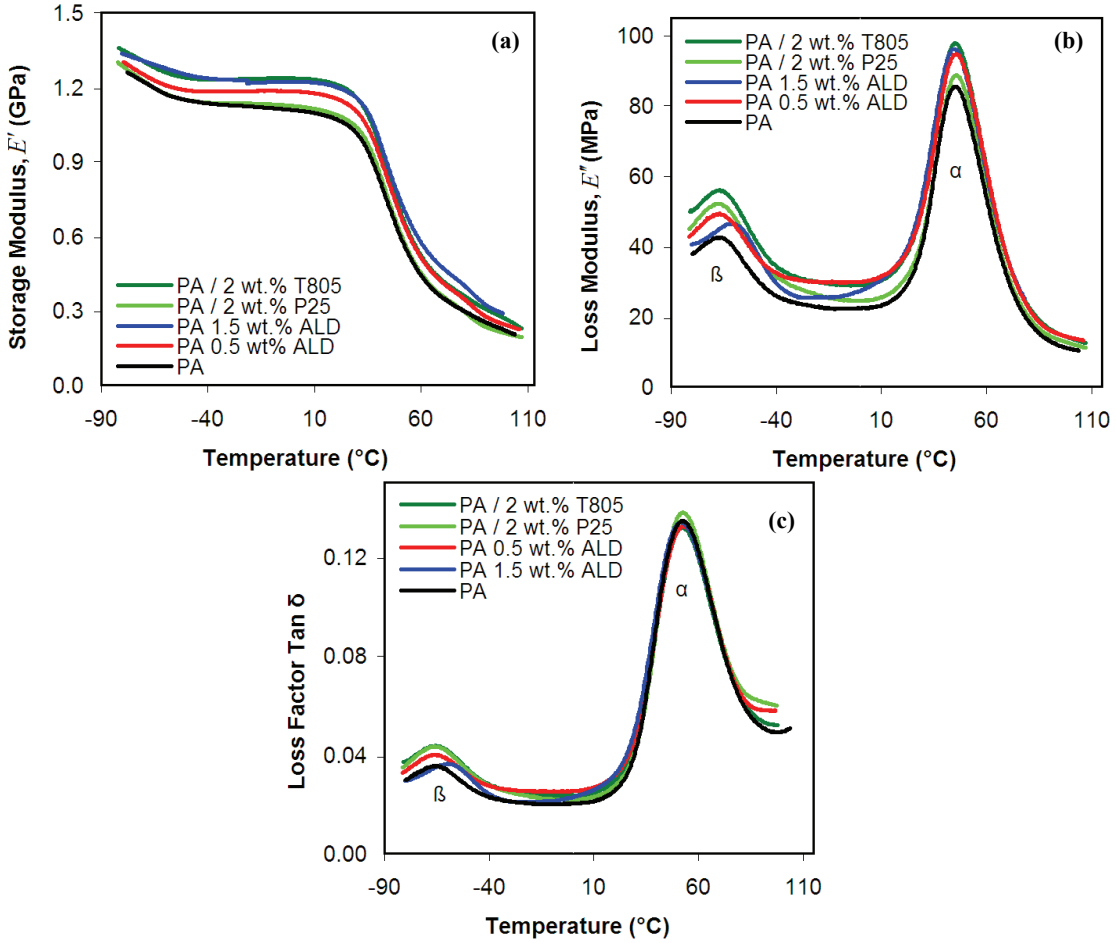

Figure 5: DMA results for (a) dynamic storage modulus, E', (b) loss modulus E'', and (c) loss factor (tan δ) as a function of temperature for PA / TiO_2 nanocomposites.

Figure 5b and 5c shows the loss modulus E'' and loss factor tan δ, respectively, versus temperature for the studied composites. Two relaxation processes are pointed out: the α a relaxation mode around 45°C associated with the mechanical manifestation of the glass transition, the ß mode near 70°C characteristic of the free amide group/water complex movements. These mechanical relaxation modes have been observed and discussed elsewhere [21]. The magnitude and temperature position of these peaks are not significantly modified by addition of TiO_2 fillers suggesting that the mobility of relaxing entities in amorphous phase of PA is not directly altered. The α peak in the loss factor tan δ (Figure 5c) is associated with T_g of PA. There is little influence of TiO_2 on it with only 0–2°C shifts towards higher temperatures. The results support well the DSC results. Consequently, DMA results suggest similar viscoelastic behavior for all studied samples and also increase of E' values for ALD-created polyamide nanocomposites at studied temperatures and, therefore, confirm that possible degradation of PA matrix is not significant. It is well recognized that E'' curves show slight broadening and magnitude increase of the viscoelastic response, for α and ß relaxation modes. Such changes are not observed in loss factor tan δ curve. As discussed above, DSC results did not yield significant crystallinity changes and therefore more intensive and boarder relaxation peaks in E'' curves are not considered to reflect the soft amorphous phase content. Consequently, such complex behaviour calls for further studies.

3.4 Dispersion of nanofiller in polymer matrix

TEM observations of the traditional TiO_2 nanocomposites proved that TiO_2 disperses well in a polymer matrix. The TiO_2 particles had a slight tendency to cluster, but the agglomerates remained typically below 100 nm with both octylsilane modified T805 TiO_2 and unmodified P25 TiO_2 (Figure 6). Identical dispersion was also suggested by similar complex viscosity curves (Figure 3b).

The morphology of the ALD-assisted nanocomposites was clearly different from that of traditional TiO_2 nanocomposites. The ALD-created TiO_2 appeared as ribbons in the PA matrix. In the PA 0.5 wt.% ALD nanocomposite, the thickness of the ribbons varied from 10 to 20 nm (Figure 6a). Further, in the PA 1.5 wt.% ALD nanocomposite, the ribbons were not only generally thicker but also varied more in their thickness (Figure 6b). Such a change in the morphology of PA TiO_2 composites could be one explanation for the decreased viscosity of PA ALD nanocomposites allowing polymer chains to slip over TiO_2 ribbons [12,14]. However, further studies, such as molecular weight determination and more systematic rheological measurements, are recommended.

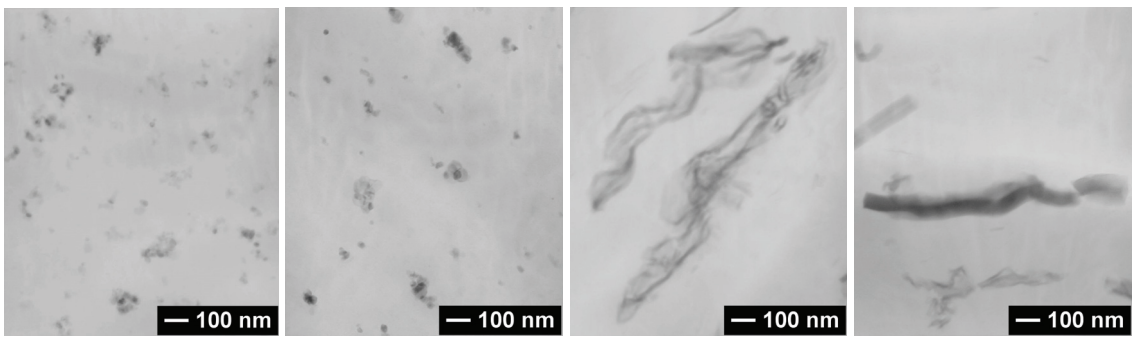

(a) (b) (c) (d)

Figure 6. TEM images of (a) PA / 2 wt.% T805, (b) PA / 2 wt.% P25, (c) PA 0.5wt% ALD, and (d) PA 1.5wt.% ALD TiO_2 nanocomposites.

4 DISCUSSION AND CONCLUSIONS

Both commercial TiO_2 and ALD-created TiO_2 polyamide composites were successfully prepared by melt-compounding. We found that melt-extruded, ALD-TiO_2-film-coated PA particles possess the following unique properties over traditionally filled nano-TiO_2 composites:

- Easy melt-processing implied by significantly lower viscosity. The complex viscosity was decreased as many as 5–10 times at certain shear rates compared to that of pure PA and traditionally filled PA.
- Good thermal properties. On adding TiO_2 to the PA matrix, χ_c, T_g, and T_m did not vary significantly compared to pure PA. Furthermore, the E' values for the ALD composites were, in fact, 7–14% higher than for pure PA. The loss factor tan δ and the E'' curves suggested very similar viscoelastic behavior for all studied sample indicating that the molecular weight of PA did not change significantly due to ALD-coating.
- Good dispersion. PA ALD composites have a unique TiO_2 ribbon structure compared to spherical clusters formed from commercial TiO_2 particles.

Consequently, ALD-created PA nanocomposite material, which possesses low melt viscosities without deteriorating the thermal properties, offers great opportunities for developing new products and markets, e.g., in the injection moulding of thin-walled micro-parts. However, intensive research is required to examine the effects of ALD coatings on different material combinations.

ACKNOWLEDGEMENTS

Financial support from Finnish Funding Agency for Technology and Innovation and The Graduate School of the Processing of Polymers and Polymer-based Multimaterials are gratefully acknowledged. We are also grateful to Ms. Sinikka Pohjonen for providing the differential scanning calorimetry and the dynamic mechanical analysis information.

REFERENCES

1- Mai Y.-W. and Yu Z.-Z. "*Polymer Nanocomposites"*, 1st edition, Woodhead Publishing Limited, 2006.
2- Ray, S.S. and Okamoto, M.,"Polymer/layered silicate nanocomposites: a review from preparation to processing", *Progress in Polymer Science*, 2003:28:1539-1641.
3- George, S.M, Ferguson. J. and Weimer A., "Atomic Controlled Layer Deposition on Particle Surfaces", *U.S. Patent 6,613,383* (Provisional Application 60/140,083(1999), 2003.
4- Spencer J.A., Liang X., George S.M., Buechler K.J., Blackson J., Wood C.J., Dorgan J.R. and Weimer. A.W., "Fluidized Bed Polymer Particle ALD Process for Producing HDPE/Alumina Nanocomposites", 2007 *ECI Conference on The 12th International Conference on Fluidization - New Horizons in Fluidization Engineering*, Vancouver, Canada, 2007: RP4: 50:417-424.
5- Liang, X., Hakim, L.F., Zhan, G.-D., McCormick, J.A., George, S.M., Weimer, A.W., Spencer, J.A., Buechler, K.J., Blackson, J., Wood, C.J. and Dorgan J.R., "Novel Processing to Produce Polymer/Ceramic Nanocomposites by Atomic Layer Deposition", *Journal of the American Ceramic Society,* 2007:90:57-63.

6- EOS GmbH, "*Product Information EOSINT P/PA2200-Pulver"*, Manufacturer Supplied Materials Data Sheet, 2008.
7- Ferguson, J.D., Yoder, A.R., Weimer, A.W. and George, S.M., "TiO_2 atomic layer deposition on ZrO_2 particles using alternating exposures of $TiCl_4$ and H_2O", *Applied Surface Science,* 2004:226:393-404.
8- Hu, Z. and Turner, C.H., "Initial Surface Reactions of TiO_2 Atomic Layer Deposition onto SiO_2 Surfaces: Density Functional Theory Calculations", *Journal of Physical Chemistry B*, 2006:110:8337-8347.
9- Degussa GmbH, "*Product Information Aeroxide TiO_2 P25 and Aeroxide TiO_2 T805"*, Manufacturer Supplied Materials Data Sheet, 2001.
10- Wypych, G., "*Handbook of Fillers*", 2nd Edition, ChemTec Publishing, Toronto, Canada, 1999.
11- Gogolewski, K. Czerniawska and M. Gasiorek., "Effect of annealing on thermal properties and crystalline structure of polyamides. Nylon 12 (polylaurolactam)", *Colloid and Polymer Science,* 1980: 258:1130-1136.
12- McNally, T., Murphy, W. R., Lew, C. Y., Turner, R. J., Brennan, G. P., "Polyamide-12 layered silicate nanocomposites by melt blending", *Polymer,* 2003: 44: 2761-2722.
13- Xu, G., Chen, G. Ma, Y., Ke, Y. and Han, M., "Rheology of a Low-Filled Polyamide 6/Montmorillonite Nanocomposite", *Journal of Applied Polymer Science*, 2008:108:1501-1505.
14- Kim G-H, Lee D-H, Hoffmann B, Kressler J, Stöppelmann G., "Influence of nanofillers on the deformation process in layered silicate/polyamide-12 nanocomposites", *Polymer*, 2001:42:1095-1100.
15- Ehrenstein G.W, Riedel, G. Trawiel, P., *"Thermal Analysis of Plastics, Theory and practice",* Hanser Publishers, Munich, 2004.
16- Kim, Y.W., Park, J.T., Koh, J.H., Min B.R., Kim, J.H., "Molecular thermodynamic model of the glass transition temperature: dependence on molecular weight", *Polymers for advanced technologies*, 2008: published online 10 March.
17- Mert, M. and Yilmazer, U., "Processing and Properties of Modified Polyamide 66-Organoclay Nanocomposites", *Journal of Applied Polymer Science*, 2008: 108:3890-3900.
18- Chiu, C.-F., Lai, S.-M., Chen, Y.-L. and Lee T.-H., "Investigation on the polyamide 6/organoclay nanocomposites with or without a maleated polyolefin elastomer as a toughener", *Polymer*, 2005:46:11600-11609.
19- Zhang, H., Zhang, Z. Yang, J.-L., Friedrich, K., "a Temperature dependence of crack initiation fracture toughness of various nanoparticles filled polyamide 66", *Polymer*, 2006:47:679-689.
20- Garciá, M., Vliet G., Cate, M. G. J., Chávez, F., Norder, B., Kooi, B, Zyl, V.E., Verweij, H. and. Blank, D.H.A., "Large-scale extrusion processing and characterization of hybrid nylon-6/SiO_2 nanocomposites", *Polymers for Advanced Technologies*, 2004:15:164-172.
21- Varlet, J., Cavaille´, J.Y., Perez, J. and Johari, G.P. "Dynamic mechanical spectrometry of nylon-12", *Journal of Polymer Science Part B: Polymer Physics*, 1990:28:2691-2705.